THE JOURNAL OF PHYSICAL CHEMISTRY Letters

Letter

pubs.acs.org/JPCL

Water–Peptide Dynamics during Conformational Transitions

Dmitry Nerukh*,† and Sergey Karabasov‡

†Nonlinearity and Complexity Research Group, Aston University, Birmingham, B4 7ET, United Kingdom

‡School of Engineering and Materials Science, Queen Mary University of London, Mile End Road, London E1 4NS, United Kingdom

Supporting Information

ABSTRACT: Transitions between metastable conformations of a dipeptide are investigated using classical molecular dynamics simulation with explicit water molecules. The distribution of the surrounding water at different moments before the transitions and the dynamical correlations of water with the peptide's configurational motions indicate that the water molecules represent an integral part of the molecular system during the conformational changes, in contrast with the metastable periods when water and peptide dynamics are essentially decoupled.

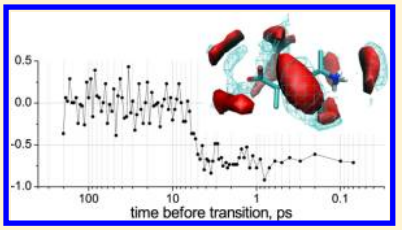

SECTION: Liquids; Chemical and Dynamical Processes in Solution

Recent investigations of protein dynamics indicate that water plays the major role in protein motion. Indeed, there is a large body of experimental and simulation evidence[1−9] showing a close connection between the water dynamics and the protein conformations. Frauenfelder and colleagues have experimentally shown that protein-dominant conformational motions are slaved by the hydration shell and the bulk solvent,[10] whereas the protein molecule itself provides an "active matrix" necessary for guiding the water's dynamics toward biologically relevant conformational changes. The change in water dynamics at the shell of up to almost a dozen water molecule diameters around proteins is found in ref 11. Very recently, a neutron scattering study demonstrated that the interfacial (hydration) water is the main "driving force" of protein dynamics governing both local and large scale motions in proteins.[12] Finally, the critical role of solvating water has been demonstrated for an important applied field of protein−ligand binding.[13]

Despite extensive research on protein dynamics, the investigations of *elementary conformational motions* are rare. The knowledge of specific molecular mechanisms, including the role of water molecules that drive the conformational moves, is highly demanded because these elementary conformational changes ultimately define all rearrangements of proteins as a whole.

In this work, we analyze molecular dynamics (MD) simulated peptide focusing on the moments of elementary conformational changes including explicit water molecules. We show that water indeed drives the changes and we elucidate the specific mechanisms of this phenomenon.

We study a zwitterion L-alanyl-L-alanine, Figure 1. This is a very convenient model because (i) the conformation of the molecule is completely defined by the two dihedral angles ψ and ϕ; (ii) in water the conformation $\psi \approx 2.5$, $\phi \approx -2.2$ radians is prevalent, however, very rare transitions to two other metastable conformations ($\psi \approx -1$, $\phi \approx -2.2$ and $\psi \approx 2.5$, $\phi \approx 1$) take place, and (iii) the transitions only happen in water

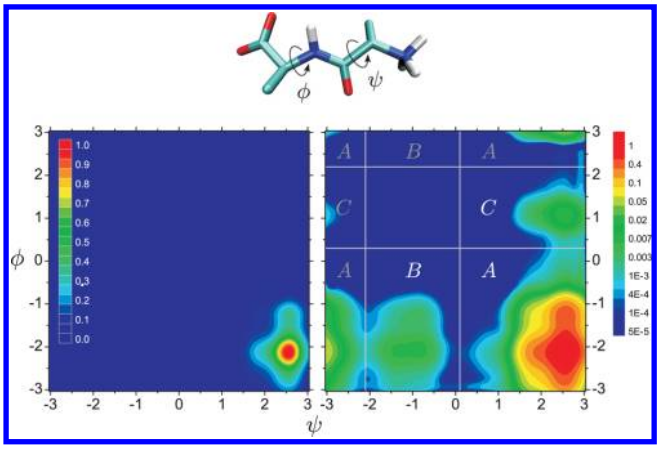

Figure 1. Top: L-alanyl-L-alanine zwitterion (GROMOS forcefield, see the Supporting Information); left: normalized probabilities of conformations (Ramachandran plot) formed by a 2 μs trajectory; right: same probabilities emphasizing the presence of two minor conformations and the partitioning for symbolization. (Similar graphs for the OPLS forcefield are in the Supporting Information.)

because in vacuum the negatively charged COO^- group strongly interacts with the positively charged NH_3^+ group, excluding all conformations except the one with the groups at the minimal distance from each other.

Two different MD models of the system (see the Supporting Information) have been studied. One is the united atom forcefield GROMOS,[14] the other is OPLS (Optimized Potentials for Liquid Simulations).[15] These are among the most popular MD models for peptides and proteins. They both show the same results in our investigations despite significantly

Received: January 8, 2013
Accepted: February 19, 2013
Published: February 19, 2013

different representation of atoms and their interactions for the peptide and water molecules.

An important conceptual point is how to define the conformational states and the moments of transitions between them. Because we are interested in the dynamical properties, we define the states as dynamically metastable states, that is, the conformations in which the molecule spends significantly more time compared with the time it spends for transitions between the conformations. This is reflected in the probabilities of the molecule's conformations calculated as the probability of finding an MD trajectory point with specific values of ψ and ϕ for the whole MD simulation time. There are three well-separated metastable states, clearly visible in the space of conformation probabilities, Figure 1. These allow one to introduce a simple natural discretization of the conformations, which we designate as '*A*', '*B*', or '*C*'.

The main goal of this work is to investigate the probability distributions of water atoms corresponding to these conformational states of the peptide. The time evolution of the water distributions during the conformational transitions between the states reflects the role of water in conformational rearrangements.

Having the conformational states *A*, *B*, and *C* defined, it is possible to identify the moments of transitions between them. The described discretization defines boundaries of the states. Thus, naively, one could define the moments of transitions between the states when the trajectory crosses the boundaries. However, the boundaries delineate the probabilities of conformations averaged over the whole trajectory. Individual pieces of the trajectory do not go directly from one state to another; instead, they wind in a complicated manner, often crossing the boundaries many times before settling in a new conformation. This results in "flickering" states when they form sequences of very short-lived alternating states, such as "...*ABABAB*...", which clearly do not satisfy the desired property of metastability. Sometimes after several such crossings, it returns to the original state without settling in the new state for long enough time. (This produces a well-known "recrossing" problem in chemical kinetics.[16−18])

The problem can be solved by increasing the time step between state observations such that the step becomes larger than the time required for the transition to complete. Thus, by discretizing time with a step Δt the continuous MD trajectory is converted into a string of symbols $\{s_i\}$, $i = 0...N$, where s_i equals '*A*', '*B*', or '*C*' depending on where the trajectory point falls at the time moment t_i and N is the number of such steps in the simulation. This sequence of symbols can be analyzed using a statistical model that, in addition to the static probabilities of the conformations, takes into account their dynamics. Such a model that has become very popular recently is the Markov State Model (MSM).[19] The model specifies the probabilities of each of the discrete states as well as the probabilities of the transitions between them. The MSM transition matrix can be calculated from the MD trajectory by counting the state changes. For the studied molecule (the GROMOS forcefield) and the time step $\Delta t = 6$ ps it is

	A	*B*	*C*
A	0.996	0.003	0.001
B	0.261	0.737	0.002
C	0.097	0.002	0.901

where the value at row i and column j gives the probability of going to state j being currently at state i. The probabilities of the states themselves are $P(A) = 0.9847$, $P(B) = 0.0074$, and $P(C) = 0.0079$. MSM provides many useful quantities describing the system.[19] In particular, it tells that the transition $A \rightarrow B$ happens once in 3.1 ns and $A \rightarrow C$ once in 9.1 ns on average.

The moments of the $A \rightarrow B$ transitions within the MSM framework are the values of t_i at which s_i is equal to B while being equal to A at the previous time moment t_{i-1}. The time precision of identifying the transitions is Δt. The MSM model is valid only for relatively large time steps, which follows from the requirement for the transitions to be history-independent (Markovian, that is, statistically uncorrelated). This requirement ensures that "flickering" is hidden from the analysis but at the same time it excludes the information about the actual process of transition. For the studied peptide, the minimal valid time step is ∼6 ps. This value is of the same order as the period of fluctuations within each conformational state and, most importantly, this is approximately the duration of the process of the trajectory passing from state to state. Therefore, the MSM has to be augmented to be able to describe the dynamics at significantly shorter time steps.

For this purpose, we build a variant of the hidden Markov model using the same conformational states of the peptide. Specifically, we use the "ε-machine" by Crutchfield et al.[20,21] (See ref 22 for recent developments in the field.) Instead of the conformational states s_i themselves we consider the l-long *sequences* of states $\overleftarrow{s}_i \equiv \{s_{i-l+1}...s_{i-2}s_{i-1}s_i\}$. The advantage of such a description is that for a small time step even if the original states are correlated over several steps, for long enough sequences $\overleftarrow{s}_i$ these new states (the sequences) are uncorrelated. We, therefore, can build a Markov model on these new states.

The resulting hidden Markov states can be classified according to their "lifetime". For example, a piece of symbolic trajectory "...*AAAAAAABBBBBBB*..." would produce a long repetition of the two-symbol state $\overleftarrow{s}_i \equiv \{AA\}$, i designating the time moments t_i, followed by one state $\overleftarrow{s}_i \equiv \{AB\}$, and then a long repetition of the state $\overleftarrow{s}_i \equiv \{BB\}$. $\{AA\}$ and $\{BB\}$ are two hidden Markov states that describe metastable conformations, whereas $\{AB\}$ is a short-lived state characterizing the details of the transition. More complex scenarios and the details of the method are given in the Supporting Information.

Using our hidden Markov model the time step can be reduced to 0.3 ps, providing a tool to investigate what happens at different moments *before* the transition including the details of the process of transition. For this, we collect the time frames at specific times before the transitions, Figure 2.

We calculate the distribution of oxygen (hydrogen) atoms in space by averaging over the selected time frames. The calculated field $f(\mathbf{x}, t)$ gives the probability of finding an oxygen (hydrogen) atom in a small volume around the location $\mathbf{x}$ at time t in advance of the transition. This probability equals the number of atoms in the small volume divided by the total number of atoms in the system. If the atoms were distributed evenly, then this number would be equal to the density of oxygen (hydrogen) divided by the atomic mass. The advantage of such probabilistic representation is that the focus is shifted away from the physical density. The calculated quantity is *not* density, as the latter is obtained by dividing the number of atoms (times their mass) by the volume. The structure of water is defined by the hydrogen bonds network, which implies approximately the same distance between water molecules

dx.doi.org/10.1021/jz400051p | J. Phys. Chem. Lett. 2013, 4, 815−819

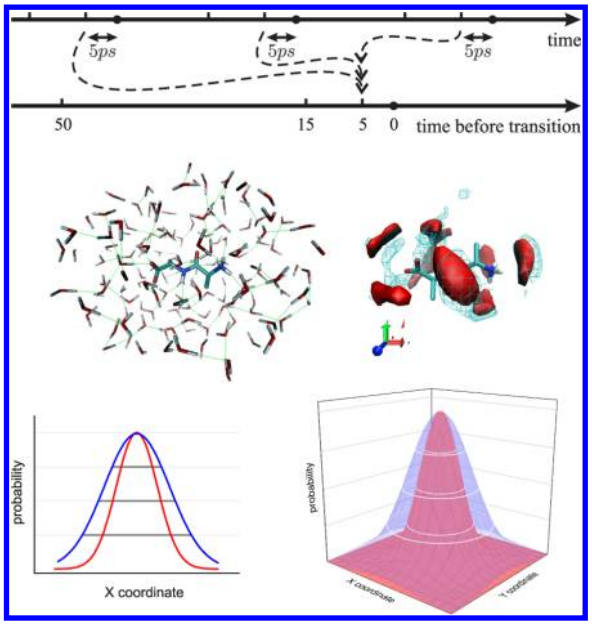

Figure 2. Top: collecting the time frames for the "time before transition" statistics; the dots on the "time" axes are the transition moments; middle, left: snapshot of the molecular system showing approximately two to three layers of water molecules hydrogen bonded with each other and the peptide; middle, right: distribution of oxygen (red, solid) and hydrogen (blue, mesh) atoms averages over the whole simulation (the isosurfaces at the probability value 0.047 (the value in the assumption of completely even distribution is 0.031) for the GROMOS model are shown); bottom: 1D and 2D probability distributions illustrating the narrowing of the peak for high probability of atoms; the red, narrower distribution describes the situation when the atoms have more specific locations rather than being more evenly distributed, as characterized by the blue distribution (see text).

everywhere (and, hence, the same local density), Figure 2, middle left. The probabilities, however, can be significantly different at different locations, indicating the preferred positions of the atoms, Figure 2, middle right. (A correct definition of local density obtained from atomistic representation of matter should be done through a function $\rho_q(\mathbf{q};\mathbf{x},t) = \Sigma_{i=1}^{N} m\delta(\mathbf{q}_i(t) - \mathbf{x})$, where $\mathbf{q} \equiv \{\mathbf{q}_1,...,\mathbf{q}_N\}$ is the set of atomistic coordinates, N is the number of atoms, m is the atom mass, $\mathbf{x}$ is the physical 3D space coordinate, t is time, and δ is the delta function. ρ_q is a function of the atom coordinates $\mathbf{q}$ that parametrically depends on $\mathbf{x}$ and t. The local density at time t is obtained by averaging over a macroscopically large volume $\Delta\mathbf{x}$: $\rho(\mathbf{x},t) = \langle\rho_q(\mathbf{q};\mathbf{x},t)\rangle_{\Delta\mathbf{x}}$. $\Delta\mathbf{x}$ defines the spatial scale. The temporal scale can also be defined by additional averaging over a time period Δt.)

The transition from conformation A to conformation B corresponds to a ~180° flip of the NH_3 group (the right-hand side of the molecule in Figure 2, middle), while during the $A \rightarrow C$ transition, the COO group rotates in similar way. Both ends of the molecule possess charges, negative on the COO and positive on the NH_3 sites, which lead to relatively strong attachment of water molecules at the ends. Hydrogen-bonded water molecules to the oxygens and to the hydrogens form the areas of high probabilities of water atoms (Figure 2, middle), indicating that, on average, it is more probable to find water atoms at those locations.

This is an intuitively clear result. More interesting is the moment just before (1−10 ps) the transitions. Water rearranges around the peptide at these times, however, we would like to stress that the rearrangement has a collective, relatively slow (compared with the motion of individual atoms) character. Water does not "give way" for the peptide atoms, rather the whole structure of surrounding water changes concurrently with the change of the average peptide conformation. There is no "dense" water around the peptide. The high probability areas show that water tends to stay at specific locations around the peptide, not that the local density (the number of atoms per unit volume) is higher. These areas indicate the peaks of probability. The broader the peaks the more even the distribution and vice versa; narrow peaks signify the preference of specific locations.

For quantifying this effect, an analogy with 1D and 2D distributions is useful (Figure 2, bottom). For the 1D distribution, the width of the peak at different levels of probability gives the measure of the tendency of atoms to be at the high probability locations. For the 2D case, the width becomes the areas of 2D regions for which the value of probability is above the chosen level, Figure 2, bottom. Finally, the 3D distribution, as in our case with molecules, can be characterized by the volumes enclosed by the isosurfaces corresponding to different levels of probability.

We have found that these volumes are significantly reduced before the transition at all levels of probability high enough to distinguish the peaks of probability around the peptide, Figure 3, left. The results for the two studied models and two transitions $A \rightarrow B$ and $A \rightarrow C$ are shown in Figure 3, right. During the time period when the rotation of the NH_3 (COO) group is most significant, from ~10 to ~1 ps, the size of the high probability areas of water is significantly reduced. This indicates that during these periods water tends to stay at more specific locations around the peptide. In other words, the flow

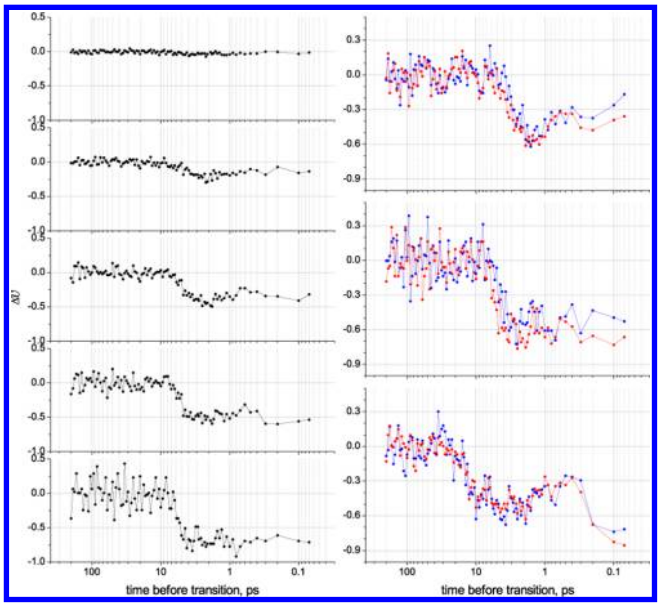

Figure 3. Left: "time before transition" dependence of the volume of the high probability areas normalized to the average values, $\Delta\nu = ((\nu - \langle\nu\rangle)/\langle\nu\rangle)$, where ν is the absolute volume (see text) and $\langle\nu\rangle$ is the volume average over the whole simulation; the isosurface areas at the probability levels of (from top to bottom) 0.013, 0.041, 0.046, 0.051, and 0.059 are shown; right: the same for oxygen (red) and hydrogen (blue) for the transition from state A to state B, GROMOS model (top), $A \rightarrow C$ transition, GROMOS model (middle), and $A \rightarrow C$ transition, OPLS model (bottom); the isosurface areas at the probability level 0.055 are shown.

dx.doi.org/10.1021/jz400051p | J. Phys. Chem. Lett. 2013, 4, 815−819

of the MD trajectories is concentrated in more narrow "channels" during the transitions.

The most informative time interval before the transition, 1−10 ps, is of the same order as the smallest possible time step for the conventional MSM (6 ps). Thus, the use of our hidden Markov model is critically important for the analysis of the details of the transitions. Figure 3, right, shows that the effect is very similar for the two studied conformational transitions and both MD models.

The overall changes of the water structure proceed concurrently with the change of the dihedral angle, reflecting the conformational transition. We can quantify the degree of the dependence between the high-probability water areas and the dihedral angles of the peptide by calculating the dynamical correlations between them. This is done using the linear stochastic estimation (LSE) technique that has a variety of use in fluid dynamics from the visualization of coherent structures in turbulent flows[23] to the identification of noise sources in turbulent jets.[24]

In the framework of LSE, the probability field $f(\mathbf{x},t)$ is decomposed into a linear combination of two parts: correlated and uncorrelated with the peptide's dihedral angles. To extract the correlated field, we first converted the $f(\mathbf{x},t)$ variable to time fluctuations by subtracting the time average: $f'(\mathbf{x},t) = f(\mathbf{x},t) - \langle f(\mathbf{x},t)\rangle_t$. Then, by considering these water fluctuations as a stochastic signal of time, a linear stochastic fit $f'_c(\mathbf{x},t) = \alpha(\mathbf{x})\phi(t) + \beta(\mathbf{x})\psi(t)$ to $f'(\mathbf{x},t)$ was computed, where $\phi(t)$, $\psi(t)$ are the mean angles at time t (that is, stochastic variables) and α and β are constants. The stochastic fit is found by minimizing the statistical error $\langle f' - f'_c\rangle_t$.[25] (See the Supporting Information for details.) $f'_c(\mathbf{x},t)$ represents the water fluctuations correlated with the peptide angles, and α and β are the coefficients of the correlations.

To find the coefficients, we solved a system of linear equations for α and β for each point of the water volume. These linear equations, which are obtained from $\langle f'(\mathbf{x},t)\phi(t)\rangle = \langle\{\alpha\phi(t) + \beta\psi(t)\}\phi(t)\rangle$ (and similarly for $\psi(t)$), are

$$\alpha\langle\phi(t)\phi(t)\rangle + \beta\langle\psi(t)\phi(t)\rangle = \langle f'(\mathbf{x}, t)\phi(t)\rangle$$

$$\alpha\langle\phi(t)\psi(t)\rangle + \beta\langle\psi(t)\psi(t)\rangle = \langle f'(\mathbf{x}, t)\psi(t)\rangle$$

The derivations are given in the Supporting Information.

The probability fluctuations field $f'(\mathbf{x},t)$ and its part correlated with the peptide's conformation $f'_c(\mathbf{x},t)$ are shown in Figure 4 for several representative time moments for the GROMOS model.

The water fluctuations (right column) are significantly stronger just before the transition (0.8 ps) compared with the stable period (~200 ps). Very surprisingly, the conditionally averaged water fluctuations (left column) are virtually uncorrelated with the peptide at all times except for the short period immediately before the transition. (Some correlations are also noticeable as early as ~5 ps before the transition, which agrees with the onset of the probability decrease in Figure 3.) Interestingly, at 0 ps, when the transition process is complete, the water probability becomes uncorrelated with the peptide, similar to the stable periods. However, the fluctuations of it remain strong, only slightly weaker than at 0.8 ps. We explain this effect by the large inertia of the water shell that needs relatively long time for the fluctuations to settle down. The fact that these post-transition water fluctuations are decoupled from the peptide emphasizes the discovered phenomenon of strong

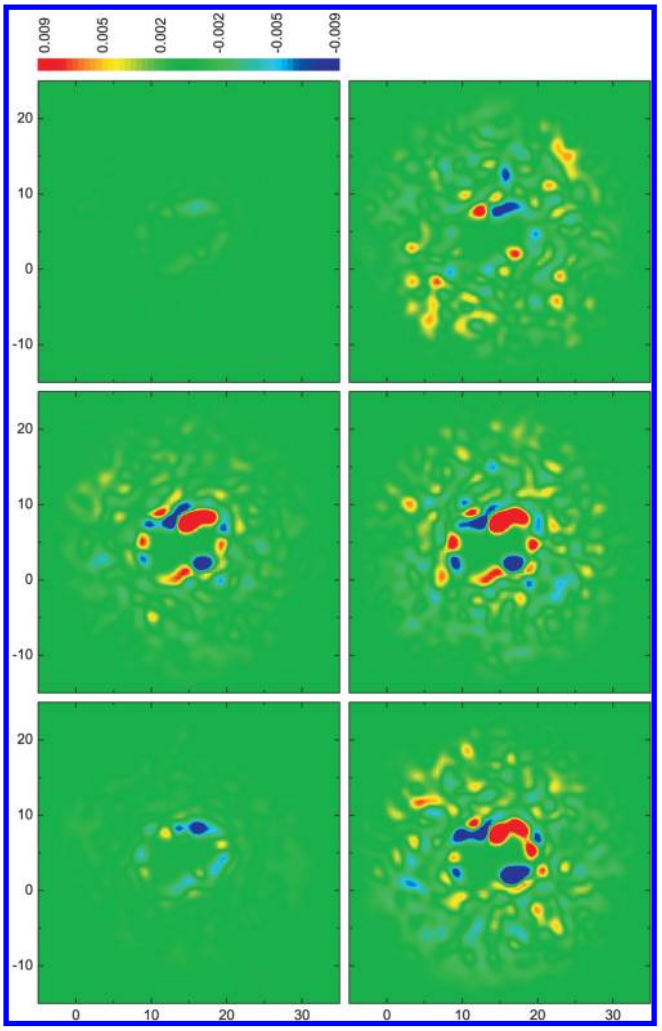

Figure 4. *xy* cross-section (the value of the *z* coordinate is chosen such that the section plane passes through the peptides's center of mass) of the probability fluctuation field $f'(\mathbf{x},t)$ (right) and its part correlated with the peptide's conformation $f'_c(\mathbf{x},t)$ (left) for oxygen. The time before transition is, from top to bottom, 200, 0.8, and 0 ps. The scale is restricted to the −0.009 to 0.009 interval for clarity; the maxima of the peaks reach the values of 0.045 and −0.041. (The results for the GROMOS model are shown; similar results for the OPLS model are given in the Supporting Information.)

water−peptide interactions precisely during the transition process.

We have found that for the OPLS model these results are very similar for the $A \rightarrow C$ transition. The $A \rightarrow B$ transition is poorly resolved for this model; therefore, the direct comparison with the GROMOS model is impossible.

In summary, we have found that (i) from 10 to 1 ps before the transition, when the dihedral angles change the most, the water molecules tend to be located at more specific positions around the peptide compared with more uniform distribution at other times; (ii) during the transition, the dynamics of water distribution becomes highly correlated with the dynamics of the dihedral angles; and (iii) these correlations are completely absent during the stable conformation periods.

We conclude that water and the peptide behave as an integral dynamical system. During the conformational transition the peptide and the surrounding water undergo transitions together. This is in contrast with the metastable periods

when their dynamics is essentially decoupled. The transition is characterized by a more specifically defined hydrogen bonds network of water reflected in more definite positions of water atoms around the peptide.

■ ASSOCIATED CONTENT

Supporting Information

Molecular model and simulation details, the hidden Markov model, the linear stochastic estimation theory, and the results for the OPLS model are provided. This material is available free of charge via the Internet at http://pubs.acs.org.

■ AUTHOR INFORMATION

Corresponding Author

*E-mail: D.Nerukh@aston.ac.uk.

Notes

The authors declare no competing financial interest.

■ REFERENCES

(1) Born, B.; Weingartner, H.; Brandermann, E.; Havenith, M. Solvation Dynamics of Model Peptides Probed by Terahertz Spectroscopy. Observation of the Onset of Collective Network Motions. *J. Am. Chem. Soc.* **2009**, *131*, 3752−3755.

(2) Pagnotta, S. E.; Cerveny, S.; Alegria, A.; Colmenero, J. The Dynamical Behavior of Hydrated Glutathione: a Model for Protein-Water Interactions. *Phys. Chem. Chem. Phys.* **2010**, *12*, 10512−10517.

(3) Johnson, Q.; Doshi, U.; Shen, T.; Hamelberg, D. Water's Contribution to the Energetic Roughness from Peptide Dynamics. *J. Chem. Theory Comput.* **2010**, *6*, 2591−2597.

(4) Zhang, L.; Yang, Y.; Kao, Y.-T.; Wang, L.; Zhong, D. Protein Hydration Dynamics and Molecular Mechanism of Coupled Water−Protein Fluctuations. *J. Am. Chem. Soc.* **2009**, *131*, 10677−10691.

(5) Ishizuka, R.; Huber, G. A.; McCammon, J. A. Solvation Effect on the Conformations of Alanine Dipeptide: Integral Equation Approach. *J. Phys. Chem. Lett.* **2010**, *1*, 2279−2283.

(6) Yeh, I.-C.; Wallqvist, A. Structure and Dynamics of End-to-End Loop Formation of the penta-Peptide Cys-Ala-Gly-Gln-Trp in Implicit Solvents. *J. Phys. Chem. B* **2009**, *113*, 12382−12390.

(7) Samuelson, S.; Tobias, D. J.; Martyna, G. J. Modern Computational Methodology Applied to the Simulation of Blocked Trialanine Peptide in Vacuo, Water Clusters, and Bulk Water. *J. Phys. Chem. B* **1997**, *101*, 7592−7603.

(8) Gaigeot, M.-P. Unravelling the Conformational Dynamics of the Aqueous Alanine Dipeptide with First-Principle Molecular Dynamics. *J. Phys. Chem. B* **2009**, *113*, 10059−10062.

(9) Li, Y.; Krilov, G.; Berne, B. J. Elastic Bag Model for Molecular Dynamics Simulations of Solvated Systems: Application to Liquid Water and Solvated Peptides. *J. Phys. Chem. B* **2006**, *110*, 13256−13263.

(10) Frauenfelder, H.; Chen, G.; Berendzen, J.; Fenimore, P. W.; Jansson, H.; McMahon, B. H.; Stroe, I. R.; Swenson, J.; Young, R. D. A Unified Model of Protein Dynamics. *Proc. Natl. Acad. Sci. U.S.A.* **2009**, *106*, 5129−5134.

(11) Ebbinghaus, S.; Kim, S. J.; Heyden, M.; Yu, X.; Heugen, U.; Gruebele, M.; Leitner, D. M.; Havenith, M. An Extended Dynamical Hydration Shell Around Proteins. *Proc. Natl. Acad. Sci. U.S.A.* **2007**, *104*, 20749−20752.

(12) Combet, S.; Zanotti, J.-M. Further Evidence That Interfacial Water is The Main "Driving Force" of Protein Dynamics: a Neutron Scattering Study on Perdeuterated C-phycocyanin. *Phys. Chem. Chem. Phys.* **2012**, *14*, 4927−4934.

(13) Limongelli, V.; Marinelli, L.; Cosconati, S.; La Motta, C.; Sartini, S.; Mugnaini, L.; Da Settimo, F.; Novellino, E.; Parrinello, M. Sampling Protein Motion and Solvent Effect During Ligand Binding. *Proc. Natl. Acad. Sci. U.S.A.* **2012**, *109*, 1467−1472.

(14) van Gunsteren, W. F.; Billeter, S. R.; Eising, A. A.; Hünenberger, P. H.; Krüger, P.; Mark, A. E.; Scott, W. R. P.; Tironi, I. G. *Biomolecular Simulation: The GROMOS96 Manual and User Guide*; Vdf Hochschulverlag AG an der ETH Zürich: Zürich, Switzerland, 1996.

(15) Jorgensen, W. L.; Tirado-Rives, J. The Opls [Optimized Potentials for Liquid Simulations] Potential Functions for Proteins, Energy Minimizations for Crystals of Cyclic Peptides and Crambin. *J. Am. Chem. Soc.* **1988**, *110*, 1657−1666.

(16) MacKay, R. S. Transport In 3d Volume-Preserving Flows. *J. Nonlinear Sci.* **1994**, *4*, 329−354.

(17) Pechukas, P. Statistical Approximations in Collision Theory. In *Dynamics of Molecular Collisions Part B*; Miller, W. H., Ed.; Plenum: New York, 1976.

(18) Chandler, D. Statistical Mechanics of Isomerization Dynamics in Liquids and the Transition State Approximation. *J. Chem. Phys.* **1978**, *68*, 2959−2970.

(19) Schuette, C.; Fischer, A.; Huisinga, W.; Deuflhard, P. A Direct Approach to Conformational Dynamics Based on Hybrid Monte Carlo. *J. Comput. Phys.* **1999**, *151*, 146−168.

(20) Crutchfield, J. P.; Young, K. Inferring Statistical Complexity. *Phys. Rev. Lett.* **1989**, *63*, 105−108.

(21) Nerukh, D.; Ryabov, V.; Glen, R. C. Complex Temporal Patterns in Molecular Dynamics: a Direct Measure of the Phase Space Exploration by the Trajectory at Macroscopic Time Scales. *Phys. Rev. E* **2008**, *77*, 036225.

(22) Crutchfield, J. P. Between Order and Chaos. *Nat. Phys.* **2012**, *8*, 17−24.

(23) Adrian, R. J. Stochastic Estimation of Conditional Structure: a Review. *Appl. Sci. Res.* **1994**, *53*, 291−303.

(24) Kerherve, F.; Jordan, P.; Cavalieri, A. V. G.; Delville, J.; Bogey, C.; Juve, D. Educing the Source Mechanism Associated With Downstream Radiation in Subsonic Jets. *J. Fluid Mech.* **2012**, *710*, 606−640.

(25) Papoulis, A.; Pillai, S. *Probability, Random Variables and Stochastic Processes*; McGraw Hill: Boston, 2002.